Journal of
Renewable Energy Research and Applications (RERA)

*Published online*

# Fault Diagnosis in Photovoltaic Modules using a Straightforward Voltage-Current Characteristics Evaluation

Arman Zare, Mohsen Simab* and Mehdi Nafar

*Department of Electrical Engineering- Marvdasht Branch, Islamic Azad University, Marvdasht, Iran.*

Received Date 05 March 2022; Revised Date 29 April 2022; Accepted Date 07 July 2022
**Corresponding author: msimab@miau.ac.ir (M. Simab)*

**Abstract**
Due to the growing demand in the electricity sector and the shift to the operation of renewable sources, the use of solar arrays has been at the forefront of the consumers' interests. In the meantime, since the production capacity of each solar cell is limited, in order to increase the production capacity of photovoltaic (PV) arrays, several cells are arranged in parallel or in series to form a panel in order to obtain the expected power. Short-circuit (SC) and open-circuit (OC) faults in the solar PV systems are the main factors that reduce the amount of solar power generation, which has different types. Partial shadow, cable rot, un-achieved maximum power point tracking (MPPT), and ground faults are some of these malfunctions that should be detected and located as soon as possible. Therefore, an effective fault detection strategy is very essential to maintain the proper performance of PV systems in order to minimize the network interruptions. The detection method must also be able to detect, locate, and differentiate between the SC and OC modules in irradiated PV arrays and non-uniform temperature distributions. In this work, based on the artificial intelligence (AI) and neural networks (NN), neutrons can be utilized, as they have been trained in machine learning process, to detect various types of faults in PV networks. The proposed technique is faster than the other artificial neural networks (ANN) methods since it uses an additional hidden layer that can also increase the processing accuracy. The output results prove the superiority of this claim.

**Keywords:** *Photovoltaic arrays, Fault detection, Machine learning, Neural Network.*

## 1. Introduction

Due to the growing need for energy resources and the reduction of fossil fuel sources, the need to keep the environment healthy, reduce air pollution, electricity, and fuel restrictions for remote rural areas, overshadows the human life. This issue makes the use of new energies such as water energy, wind energy, solar energy have a special place in the operation of the electricity network [1]. In addition, concerns about changes in the environmental conditions, along with rising oil prices, are leading to growing legislation that encourages the exploitation and commercialization of these abundant renewable resources. According to the forecast of the researchers and the International Energy Agency, the amount of electricity consumption demand, as well as the percentage of energy production in various forms, will increase rapidly and in the future. As of 1998 to 2010, the global demand for electricity increased by 50% to 27,326 TWh. On the other hand, according to scientists, by 2040, wind power and photovoltaic energy will provide 20% and 16% of the world's electricity demand, respectively [2]. Renewable energy has more advantages than other non-renewable energy sources, which the most important of them are no need for more manpower, no need for fossil fuels and more economic efficiency, continuity of energy production, higher economic efficiency in the long run, diversify energy sources, do not need a lot of water, do not pollute the environment, and even have employment opportunities if private investment is encouraged [3]. These cases in Iran in terms of vast geographical area and diversity of environment and climate in various energy sectors will always provide clear prospects for the national future. At the end of 2009, the total energy produced by PVs reached more than 21,000 MW, which is expected to reach 350 TW by 2030. Solar thermal power stations in the United States and Spain are operated by PV sources, the largest of which has a capacity of 354 MW in the Mojave Desert [4]. Therefore, protection of expensive and valuable PV sources

against all kinds of faults is considered significant, which will be discussed in this paper.

Currently, a lot of research works have been done on fault detection in PV systems. The intelligent fault detection methods in photovoltaic modules are mainly based on threshold assessment, amplitude conversion, classification methods, state evaluation or a combination of these methods [5, 6]. These methods are mainly based on the analysis of performance modes, the characteristics of the PV system, and the comparison between the measured and simulated data.

In reference [7], in order to detect a faulty PV array, the current and voltage indices are compared with their threshold values. These methods can detect faults and classify bypassed or open-circuit modules or short-circuit faults in the PV array. In another reference study [8], a simple analytical method is proposed based on a comparison between the simulated and measured reference power, taking into account the economic aspects such as reducing the number of sensors. This method can only detect the number of shorted or open-circuit modules in the PV array. The diagnostic scheme presented in [9] is based on monitoring and comparing the measured DC and AC power with the simulated power to reveal the type of fault in the PV array and inverter. This method can locate the disconnected PV array but cannot locate the disconnected modules in the array. Cost reduction using the least number of sensors in reference [10] is also considered to detect the number of shorted or open-circuit modules and to be distinguished from modules that are in partial shadow. The diagnostic method [11] is customized based on array voltage monitoring and comparison with training information. However, different PV installations and different environmental conditions require different training information, which is very difficult to obtain. Some other fault detection strategies are comparisons of simulated V-I curves and laboratory PV systems [12, 13] but the threshold for comparative purposes has not been considered. For example, in [14], only OC fault is considered. On the other hand, some fault detection techniques based on I-V specifications in [15, 16] have examined the threshold limits. A set of fault thresholds is defined in [17] to detect the occurrence of faults in the PV array but this method cannot distinguish between SC faults and partial shadows. Reference [18] provides a threshold fault detection method in different cloud conditions. In reference [19], the authors have used artificial neural network (ANN) along with threshold analysis to identify the faults that have common features. However, the location of faulty modules in these V-I curve-based methods has not been investigated. In that paper, machine learning technique is applied for regular health monitoring of PV system. Software simulation is used to model the temperature dependent relation for the series resistance and ideality factor, which is used as a classifier for fault identification. The simulation results demonstrate the high accuracy of the proposed fault classifier. In [20], the authors propose a novel artificial neural network model for fault identification but ANN is less suitable because error might be high in some cases, while high accuracy is the most important factor to be considered; while in [21], the author applied latterly primed adaptive resonance theory neural network algorithm for identification of fault at module level. The said algorithm can interpret both smooth and perturbed behavior of PV caused by cloud cover or etc. The author detected line to line fault by employing multi-resolution signal decomposition and two-stage support vector mechanism. The proposed technique is economical because it only requires measurement of voltage and current. Trained by a minimum portion of data, this algorithm presents a satisfactory accuracy in detecting L-L faults under different operating conditions. In addition to above, they have used MPPT based sensor less fault detection technique but it was not reliable and very less accurate.

Based on the explanations provided, this paper will present a method that, based on artificial intelligence and neural networks, neutrons can use, as they have been trained in machine learning, to detect various types of faults in photovoltaic networks. This method is faster than other artificial network methods because it uses an additional hidden layer that can also increase the processing accuracy. The output results prove the truth of this claim. In this manuscript, the authors have used the radial basis function (RBF) neural network, in which this method is not mentioned in [23]. In mathematical modeling, RBF is an artificial neural network that uses radial basis function as activity functions. The output of this network is a linear combination of radial basis functions for the input and neuron parameters. These networks are used in approximation, time series prediction, classification, and system control functions. The RBF networks usually consist of three layers: the input layer, the hidden layer with a non-linear RBF activity function, and the output layer. The input can be modeled as a vector of real numbers, and the output of this

network is a scalar function of the input vector. The RBF networks are usually trained by a two-step algorithm. In the first step, the central vectors for the RBF functions in the hidden layer are selected. The second step is simply fitted to a linear model with uncertain coefficients for the hidden layer outputs according to the objective function. Finally, this neural network can extract the system model very powerfully.

This paper is presented as what follows. Introduction will be provided in Section 1. Section 2 describes the common types of faults in PVs and their classification. Sections 3 and 4 examine the algorithm for solving the problem by introducing ANN. Section 5 is devoted to case studies, and finally, in Section 6, conclusions will be expressed.

## 2. Fault types in PV systems

In the solar system, faults can be divided into two general types: PV side faults and DC network side faults. When potential faults occur in the system, the efficiency of the power plant is degraded. The faults in the PV solar system are divided into three main types: PV array faults, MPPT faults, and DC-DC converter faults [20].

The PV array fault consists of two main parts: panel fault and cabling fault. The most common types of faults in the ground panel/module are ground fault, bridge fault, open-circuit fault, and non-compliance fault.

### 2.1. Earth fault

Earth fault occurs when a current flow creates an abnormal path to earth. Two types of ground must be considered for the PV system such as grounding the system and grounding the equipment. In grounding the system, a negative conductor is grounded among the fault protection equipment. Metal parts without displacement of PV module frames, electrical equipment, and conductor enclosures must be included in the grounding of the equipment.

### 2.2. Bridge fault

The bridging fault occurs when a weak connection between two points with different potentials in the module or cabling field is detected. Failure of cable insulation due to chewing of cable insulation by animals, mechanical damage, water ingress or corrosion can cause these faults.

### 2.3. Open-circuit fault

An open-circuit fault occurs when one of the current paths in the series of loaded paths is broken or opened. Poor connection between cells, disconnection, and connection of connectors in junction boxes or failure of wires can cause this fault.

### 2.4. Compliance fault

Non-compliance will occur in PV modules when the electrical parameters of one or a group of cells change relative to other cells. This fault causes irreversible damage to the PV modules and loss of power.

### 2.5. Cable fault

Bridge faults, open circuit faults, and ground faults occur in the carriers of power lines and cabling systems. This perennial junction box on the back of a solar panel or in the corner and the cable bends can cause this fault.

### 2.6. MPPT fault

MPPT increases the power fed to the grid from the PV array. The MPPT function is degraded when a fault occurs in the charge regulators. Since a fault occurs in MPPT, the output voltage and output power decrease, accordingly.

### 2.7. Fault in DC-DC converter

The DC-DC converters convert DC power from one voltage level to another. Power semi-conductor switches are one of the most failed parameters, which are caused by factors such as changing environmental conditions, system instability, heavy load, thermal/power cycles, and manufacturing defects.

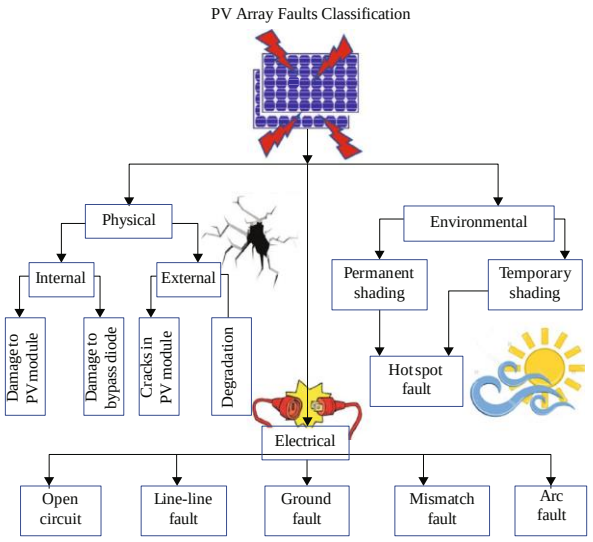


**Figure 1. Comprehensive PV array fault classification.**

### 2.8. Fault on DC network side

In the DC network, two types of faults can be identified. General blackout that is unbalanced

due to an external fault in the system, light, and voltage or power outage due to a defect in the DC section such as a weak switch, overcurrent or overvoltage.

Another classification can be represented in figure 1, while some of most usual faults occurring in PVs are demonstrated and addressed in figure 2.

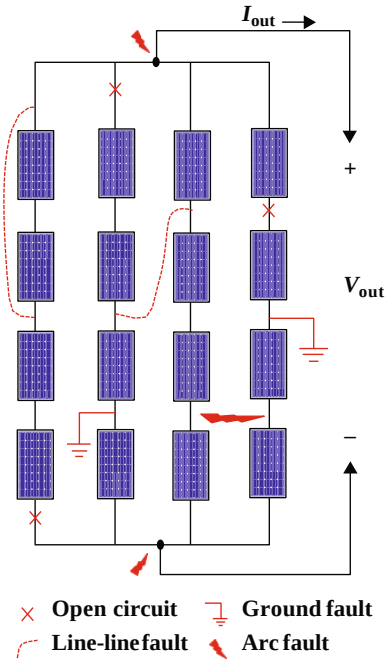


**Figure 2. Most usual faults occur in PVs based on their location.**

## 3. Machine learning and ANN

Machine learning is a subset of artificial intelligence that allows systems to learn and progress automatically without explicit programming. The main focus of machine learning is on the development of computer programs that can access data and use it for their own learning. The learning process begins with observations or data such as examples, direct experiences or instructions to arrive at a pattern in the data and make better decisions based on the examples we provide. The main goal is to allow the computer to learn automatically without human intervention and to be able to adjust its actions accordingly. The main framework of machine learning process-based ANN is depicted in figure 3.

Machine learning algorithms are mainly classified into two types: supervised and unsupervised. The monitored machine learning algorithm can use what it has learned in the past, as well as new tagged data, to predict the future. While it starts with training data set analysis, the learning algorithm produces an inferential function to make predictions about the output values. This type of system is able to determine the target for each new data after a sufficient training. This learning algorithm can also compare its output with the correct and pre-determined output, and find the existing faults to correct the model accordingly.

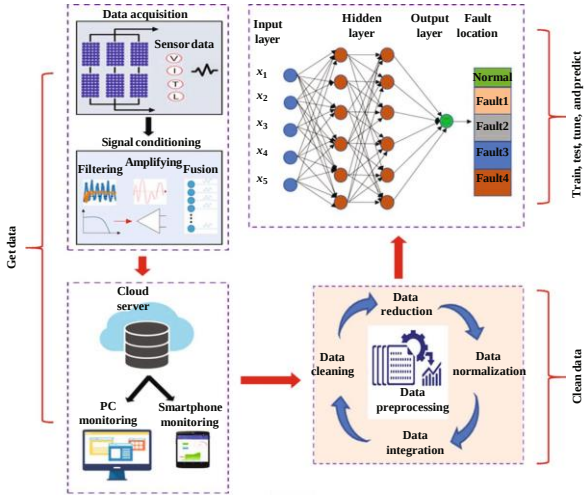


**Figure 3. Main framework of machine learning process-based ANN.**

In contrast, unsupervised machine learning algorithms are used when the information required for training is neither categorized nor labeled. Unsupervised learning studies how a system can deduce the description of a hidden structure from unlabeled data. This type of system does not specify the appropriate output, and can only explore data and infer hidden structures from unlabeled data.

The semi-supervised machine learning algorithm is between the previous two types. This system uses both labeled and unlabeled data types for training. Systems that use this method can significantly improve learning accuracy. We usually choose this type of learning when the labeled data obtained requires skilled and relevant resources for teaching and learning; otherwise, access to labeled data usually does not require additional resources.

Amplifier machine learning algorithms are a way of interacting with their environment through actions and detecting faults and rewards. Trial, fault detection, and delay rewards are the most important features of reinforcement learning. This type of learning allows machines and software agents to automatically determine their ideal behavior to maximize their performance. The system uses simple reward feedback to see which action is best, and this is known as a boost signal.

Machine learning enables the analysis of large amounts of data. Learning to identify profitable or risky opportunities usually yields faster and more

accurate results but training may require additional time and resources. A combination of machine learning and artificial intelligence and cognitive technologies can be effective in processing large amounts of information.

## 4. ANN for fault detection

The neuron, as the smallest unit of data processing in an artificial neural network, represents the basis of its performance behavior. It is made up of a combination of several neurons, which depending on the type of cell have a specific task in the network. How nerve cells connect in different layers determines the network structure, which is called the network architecture. The structure of each neural network is such that it is located in the input layer of the receiving cells and in the middle (hidden) layers of the processing cells. The output layer also contains cells that, in addition to processing connections, also show the network response. The grid layers are connected by attachments of different weights. The following figure shows the general structure of a neural network.

The function, as shown in figure 4, is such that from the sum of the product of the input matrix *P* with elements *P* (i = 1, 2, … r) and the weight matrix *W* with elements *W* (i = 1, 2, … r) attributed to each of the neuron input junctions and a constant value of 1 with weight *b*, results in a specific neuron input n as equation (1) [21].

$$n = \sum_{i=1}^{r} P_i \, W_{1,i} + b = WP + b \tag{1}$$

In the above relation, *r* is called the input number, and *b* is called the oblique weight of the neuron. Finally, the output of the neuron will be as follows:

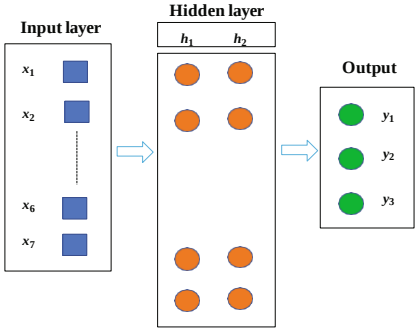


**Figure 4. ANN structure [22].**

$$a = f(WP + b) \tag{2}$$

The parameters *W* and *P* are adjustable, and the function *f* is selected by the designer. By choosing a suitable structure or the correct architecture of the network, i.e. placing the principles and correctness of all components and introducing the function of the activity and its appropriate training law, the network can be trained to achieve the desired goal and receive the desired behavior and response.

Radial basis function networks typically have three layers: an input layer, a hidden layer with a non-linear RBF activation function, and a linear output layer. The input can be modeled as a vector of real numbers $x \in R^n$. The output of the network is then a scalar function of the input vector, $\varphi : R^n \rightarrow R$, and is given by:

$$\phi\,(x) = \sum_{i=1}^{N} a_i \rho\left(||x - c_i||\right) \tag{3}$$

where *N* is the number of neurons in the hidden layer, $c_i$ is the center vector for neuron *i*, and $a_i$ is the weight of neuron *i* in the linear output neuron. Functions that depend only on the distance from a center vector are radially symmetric about that vector, hence the name radial basis function. In the basic form, all inputs are connected to each hidden neuron. The Gaussian basis functions are local to the center vector in the sense that:

$$\lim_{||x|| \rightarrow \infty} \rho\left(||x - c_i||\right) = 0 \tag{4}$$

Given certain mild conditions on the shape of the activation function, the RBF networks are universal approximators on a compact subset of $R^n$. This means that an RBF network with enough hidden neurons can approximate any continuous function on a closed, bounded set with arbitrary precision. The parameters $a_i$, $c_i$, and $\beta_i$ are determined in a manner that optimizes the fit between φ and the data.

In addition to the above normalized architecture, the RBF networks can be normalized. In this case, the mapping is:

$$\phi\,(x) \cong \frac{\sum_{i=1}^{N} a_i \rho\left(||x - c_i||\right)}{\sum_{i=1}^{N} \rho\left(||x - c_i||\right)} \tag{5}$$

Therefore:

$$\phi\,(x) \cong \sum_{i=1}^{N} a_i u\left(||x - c_i||\right) \tag{6}$$

where:

$$u\left(||x - c_i||\right) = \frac{\rho\left(||x - c_i||\right)}{\sum_{i=1}^{N} \rho\left(||x - c_i||\right)} \tag{7}$$

Equation (7) is known as a normalized radial basis function.

### 4.1. Layers

The general structure of a multi-layer post-diffusion network is shown in figure 5. In the neural network shown, an input layer (X units), a layer containing hidden units (W units), and an output layer (Y units) are shown. As shown in this figure, the output and hidden units can also have bias.

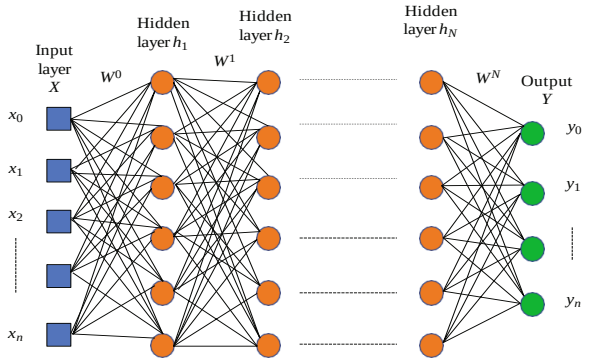


**Figure 5. General structure of a multi-layer ANN network.**

The bias is denoted by $y_k$ with $w_k$, and the bias is denoted by negative $z_j$ with $v_j$. These biases act like input weights on connections from units whose output is always 1. In this figure, only the direction of information flow for the feed forward phase of the operation is shown. In the post-learning phase, the signals are sent in the opposite direction from the output layer to the input layer.

### 4.2. Post-release algorithm

In the feed stage, each input $X_i$ receives an input signal and sends these signals to each of the units $h_1$, …, $h_p$. Each hidden unit then calculates its activation and sends its signal, $h_i$, to all output units. Each output unit calculates its activation $Y_k$ equal to $y_k$ to form the network response to the proposed input pattern.

In monitoring training for each input pattern, a target value is also available. During the post-propagation instruction, each unit compares its calculated $y_k$ output with its target value, $t_k$, to determine the corresponding fault of that pattern for that unit. Based on this fault, the factor $d_k$ where $k = (1, …, m)$ is calculated. The $d_k$ factor is used to distribute the fault value of the $y_k$ output unit to all units of the previous layer (hidden units connected to $Y_k$). In the weight adjustment step, this factor is used to update the weights between the output layer and the hidden layer. Similarly, the $d_j$ factor that $j = (1, …, p)$ is calculated for each hidden unit $W_j$. The $d_j$ is only used to update the weights between the hidden layer and the output layer, and we do not need to transfer the hidden layer fault to the input layer.

Once all d factors have been determined, the grid weights for all layers are adjusted simultaneously. The weight of $w_{jk}$ (weight of hidden unit $h_j$ to output unit $y_k$) is adjusted based on the $d_k$ factor and activation of the hidden factor $h_j$. Adjusting the weight of $v_{ij}$ (weight of input unit xi to hidden unit $h_j$) is based on the $d_j$ factor and activation of input unit, $x_j$.

### 4.3. Training algorithm

Each one of the activation functions defined in the previous section can be used in the standard post-emission algorithm. The shape of the data, especially the target values, is an important factor in choosing the activation function. Due to the the simple relationship between the value of the function and its derivative, there is no need to calculate the exponential part of the derivatives in the post-propagation phase of the algorithm. The post-publication training algorithm is as follows:

1- We give the initial values to the weights (select small random values).

2- We do steps 3 to 10 until the stop conditions are met.

3- For each training pair (input values and target), we perform steps 4 to 9.

4. Each input unit $X_i$ receives the input signal xi and distributes it to all units in the next layer (hidden units).

5. Each hidden unit $W_j$ sums up its weighted input signals, and uses its activation function to calculate the output signal.

6. Each $Y_k$ output unit sums up its weighted signals, and uses its activation function to calculate the output signal.

7. Each $Y_k$ output unit receives the target pattern corresponding to the input training pattern, and calculates the fault.

8. Each secret unit $W_j$ sums its delta inputs, and multiplies it by its activation function derivative to calculate the fault information parameter.

9. Each $Y_k$ output unit will update its weights and biases, and each hidden $W_j$ unit will also update its biases and weights.

10. We check the stop conditions.

### 4.4. Training duration

Since the main motivation for using a post-release network is to achieve a balance between giving the correct response and the trained algorithms to the network and generating the right response to

the new patterns, continuing network training when the amount of squares of fault is minimized is not necessarily useful. For this purpose, it is suggested to use two separate datasets for training-testing. Weight change in the network is based on training data and at intervals during training; network fault is calculated for training-the test data. Accordingly, training will continue until the amount of training-test data fault is reduced during training. As network fault begins to increase, the network clearly begins to maintain training patterns and gradually loses its generalizability. At this stage, the training ends.

## 5. Simulation Results

The paper presented in reference [23] is a review report of the fault detection methods in photovoltaic arrays, which in total, examines their advantages and disadvantages. No simulations were performed in that paper, and only the comparison of fault checking methods were sufficient to be presented. However, in the present manuscript, the authors, using artificial intelligence and machine learning, have investigated the different faults in PV arrays and presented several simulations in different cases. These case studies conducted show that the proposed method detects the fault location and its type more accurately than the previous methods, where the faulty section of the power grid could be disconnected from the other healthy network areas.

When different faults emerge in a PV array, the corresponding output characteristics of the PV array are entirely different. The output characteristic curves of the PV array under fault types are shown as figure 6. As shown in this figure, when an open-circuit fault occurs, the short-circuit current of the PV array decreases significantly; when a short-circuit fault appears, the open-circuit voltage of the PV array reduces rapidly; when the PV array is partially shaded, the MPP current of the PV array declines obviously but the short-circuit current and the open-circuit voltage of the PV array are basically invariant; when a degradation fault emerges, the MPP current and voltage of the PV array are reduced compared with the PV array fault-free status, and it is worth noting that the short-circuit current and the open-circuit voltage of the PV array remain unchanged. According to the above analysis, the output variables of the voltage and current at MPP, the short-circuit current and the open-circuit voltage of the PV array happen corresponding to changes under different fault conditions.

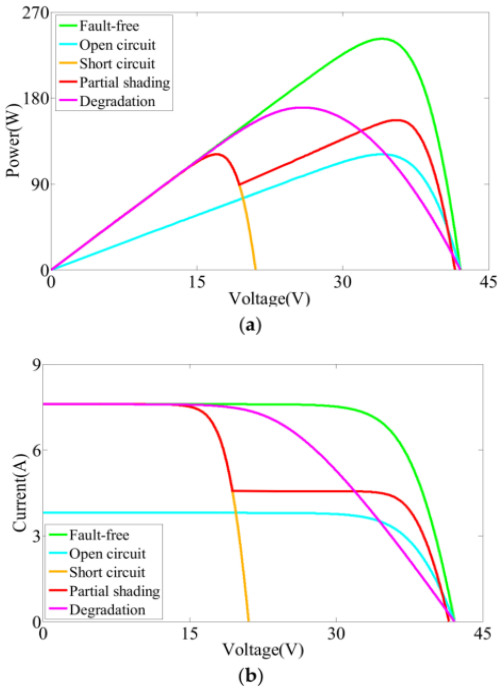


**Figure 6. Output characteristic curves of PV array under common fault conditions (a) power-voltage curves; (b) current-voltage curves.**

Before creating a database, several faults are applied one by one in any voluntary place of a PV array, and their voltage and current output are plotted and stored as VI characteristics. Then using the RBF neural network, many multi-layered educations are performed on the input data to compare which training method works properly. In these training process, the accuracy and Gaussian function used are changed in order to the best trained system is obtained. After accessing the trained system, any fault that is applied to the input, with acceptable accuracy, the amount of damaged modules and the fault current are identified, as well as the location of the fault.

It is worth mentioning that the database for each system is determined according to the specifications of the same system, and no external database will be used.

For this purpose, a comparison is made between different neural network methods in identifying the system.

### 5.1. Method one

At this stage, the Levenberg-Marquardt neural network with 50 layers is selected. The performance diagram of this network is shown in figure 7. It is observed that the computational error is calculated to be about 3.7%. Therefore, due to a high estimation error, this neural network model is not used.

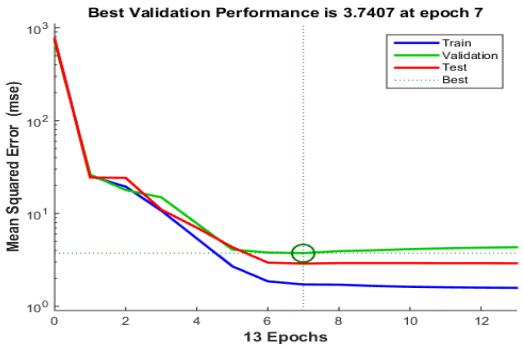


**Figure 7. Levenberg-Marquardt neural network performance.**

## 5.2. Second method

At this stage, a 50-layer Bayesian neural network is used. The performance of this neural network model is shown in figure 8. The estimation error in this case is 2.5%, which again due to the increase of the practical test error, this network will also be excluded.


**Figure 8. Bayesian neural network performance.**

## 5.3. Third method

At this stage, a 50-layer Scaled Conjugate Gradient neural network is used. Considering that, the estimation error is 1.7%, and this amount of error is not acceptable in education, as shown in figure 9.

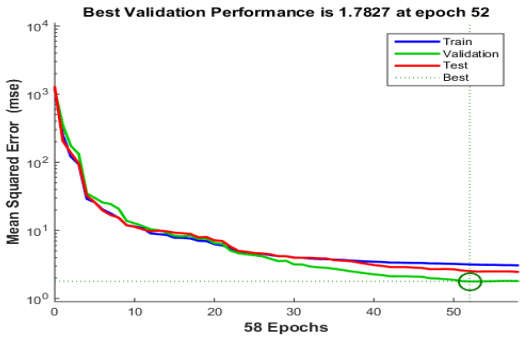


**Figure 9. Conjugate Gradient neural network performance.**

## 5.4. Proposed method

At this stage, the Radial Basis Function neural network is used. In this case, we set the prediction error to 0.1% (this feature does not exist in the previous triple neural networks) and run the simulation. The network performance diagram is shown in figure 10. It is observed that after about 750 epochs, the necessary convergence is achieved, and the RBF neural network is generated.

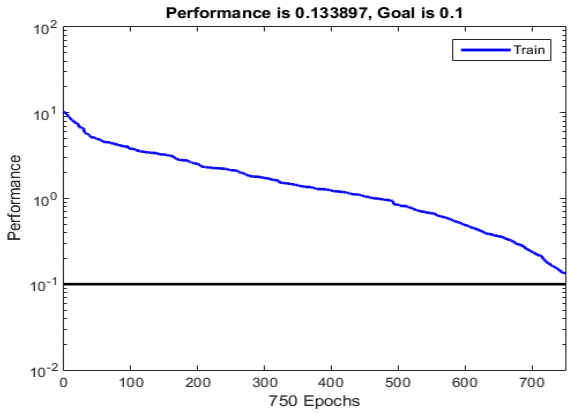


**Figure 10. RBF neural network performance.**

## 5.5. Power system model

In order to evaluate the effect of the neural network, PV is tested with an internal LL fault. Power generation data in this case study is shown in figure 11. The first neural network training is done with the same power data, which is shown in the blue diagram in the figure. It is observed that the training results are almost consistent with the actual data, and the proposed neural network provides a wide up and down band for modeling.

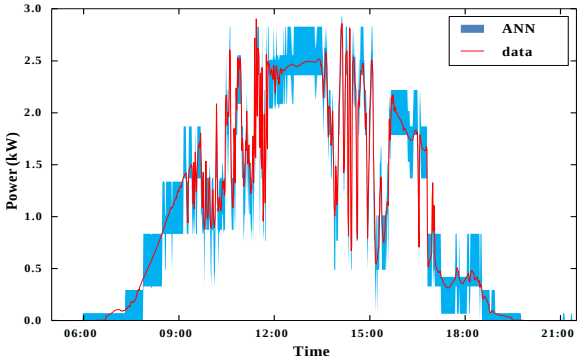


**Figure 11. PV output power comparison for data and ANN.**

The trained algorithm was then applied to data collected in [23], that contained fault conditions. Each one of these changes in the temporal data was identified by the ANN algorithm and was flagged in the bottom graph of figure 12. The current and power dropped significantly due to cloud cover at time 14:44 but were recognized by the ANN algorithm as a normal behavior. Each of the tests conducted produced no false positives or false negatives. Therefore, the probability of false

alarm and detection were equal to 0% and 100%, respectively.

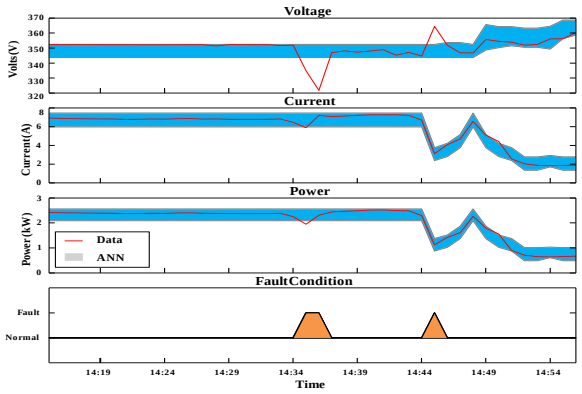


**Figure 12. Voltage, current, and power of PV array in fault condition interval.**

The second experiment used data produced by a component-based model. The model was able to represent the actual operations well, as described in figure 12. This figure compares the voltage, current, and power outputs for the model and actual system on [23]. It is evident that the model is able to predict current and power with a high accuracy but was not able to represent voltage as well. Additionally, figure 13 plots the fault condition simulated in the model. Similar to the actual sensor data, the model experiences a drop in voltage, current, and power. The accuracy of the model is defined in more detail within the scatter plots shown in figures 14 and 15 for voltage and current, respectively. The distribution of the voltage scatter plot did not match well with the ideal y = x line and produced a low $R^2$ of 0.47. The current and power scatter plots described a sufficient match each with an $R^2$ equal to 0.99. In addition the linear fit line for each matched very close to the ideal y = x line [23].

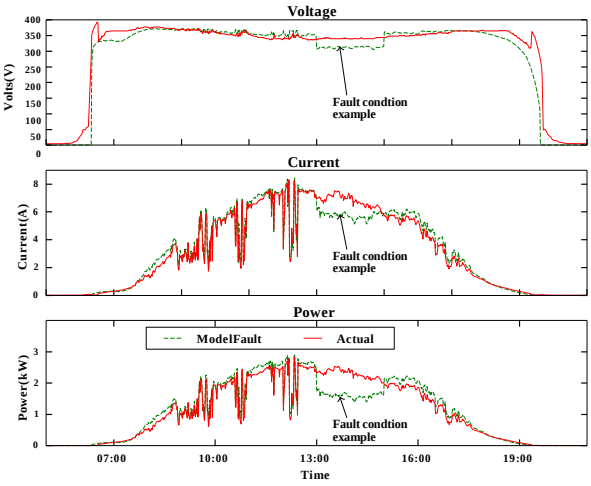


**Figure 13. Voltage, current, and power of PV array for fault detection.**

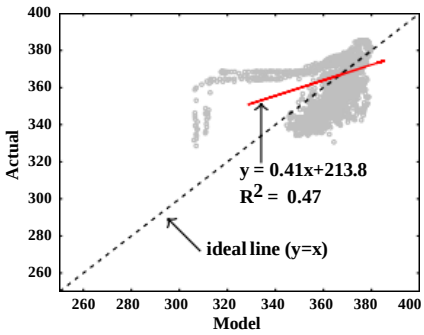


**Figure 14. Voltage scattered plot.**

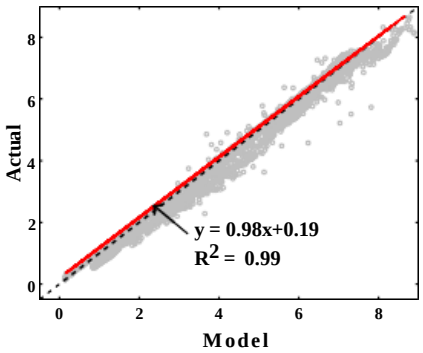


**Figure 15. Current scattered plot.**

For other simulation results, in order to investigate the various types of faults and the extent of their detection in the power system including photovoltaic sources, the errors of the case studies performed are given in table 1. In this table, where the accuracy of fault detection has been evaluated using various methods, it can be concluded that the RBF neural network will be more powerful than all the available methods.

**Table 1. Comparison between error percentage of existing neural network methods and proposed method.**

| Fault types | Approaches | | | |
|---|---|---|---|---|
| | Levenberg-Marquardt NN | Bayesian NN | Conjugate Gradient NN | RBF |
| Open circuit | 7.852 % | 7.125 % | 6.953 % | 3.462 % |
| Partial shadow | 12.912 % | 11.724 % | 9.421 % | 6.235 % |
| LG | 3.451 % | 3.021 % | 2.421 % | 0.602 % |
| LL | 3.825 % | 3.152 % | 2.957 % | 0.645 % |
| LLG | 3.119 % | 2.532 % | 1.886 % | 0.442 % |
| LLLG | 3.342 % | 2.868 % | 1.996 % | 0.324 % |

## 6. Conclusion

In this paper, a complete framework for predicting internal photovoltaic fault based on training and neural network was presented. Since internal faults can occur in multiple instances, it is important to classify them and determine the exact location of the fault in the PV array. In this work, the LL fault was investigated, and in the case

studies, it was observed that the proposed neural network responded rapidly to changes in voltage and current at fault intervals. Since the time of the fault is known, the exact location of the arrays is determined, and the operation of the network is informed according to the instructions previously implanted in the neural network by machine learning. In the proposed technique, in the fault intervals, a lot of training can be given to the neural network and prepare it for different types of poor system performance. Since the IV and PV curves are the best characteristics for finding faults in PV arrays, so in the tutorials, these two curves are enough, and then voltage and current distribution diagrams are drawn. The current voltage regression can accurately detect the location and types of faults at appropriate times without the use of a neural network.

## 7. References

[1] Ahmadi, A. and Ehyaei, M. (2020). Development of a Simple Model to Estimate Entropy Generation of Earth. Renewable Energy Research and Applications, 1(2), 135-141.

[2] Alayi, R. and Jahanbin, F. (2020). Generation management analysis of a stand-alone photovoltaic system with battery. Renewable Energy Research and Application, 1(2), 205-209.

[3] Pourderogar, H., Harasii, H., Alayi, R., Delbari, S. H., Sadeghzadeh, M., and Javaherbakhsh, A. R. (2020). Modeling and technical analysis of solar tracking system to find optimal angle for maximum power generation using MOPSO algorithm. Renewable Energy Research and Application, 1(2), 211-222.

[4] Kamari, M., Isvand, H., and Alhuyi Nazari, M. (2020). Applications of multi-criteria Decision-making (MCDM) Methods in Renewable Energy Development: A Review. Renewable Energy Research and Applications, 1(1), 47-54.

[5] Pillai, D. S. and Rajasekar, N. (2018). Metaheuristic algorithms for PV parameter identification: A comprehensive review with an application to threshold setting for fault detection in PV systems. Renewable and Sustainable Energy Reviews, 82, 3503-3525.

[6] Dhimish, M., Holmes, V., Mehrdadi, B., and Dales, M. (2018). Comparing Mamdani Sugeno fuzzy logic and RBF ANN network for PV fault detection. Renewable energy, 117, 257-274.

[7] Pillai, D. S., Blaabjerg, F., and Rajasekar, N. (2019). A comparative evaluation of advanced fault detection approaches for PV systems. IEEE Journal of Photovoltaics, 9(2), 513-527.

[8] Li, B., Delpha, C., Diallo, D., and Migan-Dubois, A. (2021). Application of Artificial Neural Networks to photovoltaic fault detection and diagnosis: A review. Renewable and Sustainable Energy Reviews, 138, 110512.

[9] Fadhel, S., Delpha, C., Diallo, D., Bahri, I., Migan, A., Trabelsi, M., and Mimouni, M. F. (2019). PV shading fault detection and classification based on IV curve using principal component analysis: Application to isolated PV system. Solar Energy, 179, 1-10.

[10] Madeti, S. R. and Singh, S. N. (2018). Modeling of PV system based on experimental data for fault detection using kNN method. Solar Energy, 173, 139-151.

[11] Appiah, A. Y., Zhang, X., Ayawli, B. B. K., and Kyeremeh, F. (2019). Review and performance evaluation of photovoltaic array fault detection and diagnosis techniques. International Journal of Photoenergy, 2019.

[12] Dhoke, A., Sharma, R., and Saha, T. K. (2019). An approach for fault detection and location in solar PV systems. Solar Energy, 194, 197-208.

[13] Pillai, D. S. and Rajasekar, N. (2018). An MPPT-based sensorless line–line and line–ground fault detection technique for PV systems. IEEE Transactions on Power Electronics, 34(9), 8646-8659.

[14] Dhibi, K., Fezai, R., Mansouri, M., Trabelsi, M., Kouadri, A., Bouzara, K., ... and Nounou, M. (2020). Reduced kernel random forest technique for fault detection and classification in grid-tied PV systems. IEEE Journal of Photovoltaics, 10(6), 1864-1871.

[15] de Oliveira, A. K. V., Aghaei, M., and Rüther, R. (2020). Aerial infrared thermography for low-cost and fast fault detection in utility-scale PV power plants. Solar Energy, 211, 712-724.

[16] Rouani, L., Harkat, M. F., Kouadri, A., and Mekhilef, S. (2021). Shading fault detection in a grid-connected PV system using vertices principal component analysis. Renewable Energy, 164, 1527-1539.

[17] Abbas, M. and Zhang, D. (2021). A smart fault detection approach for PV modules using Adaptive Neuro-Fuzzy Inference framework. Energy Reports, 7, 2962-2975.

[18] Jaskie, K., Martin, J., and Spanias, A. (2021). PV Fault Detection Using Positive Unlabeled Learning. Applied Sciences, 11(12), 5599.

[19] Bakdi, A., Bounoua, W., Guichi, A., and Mekhilef, S. (2021). Real-time fault detection in PV systems under MPPT using PMU and high-frequency multi-sensor data through online PCA-KDE-based multivariate KL divergence. International Journal of Electrical Power & Energy Systems, 125, 106457.

[20] Triki-Lahiani, A., Abdelghani, A. B. B., and Slama-Belkhodja, I. (2018). Fault detection and monitoring systems for photovoltaic installations: A review. Renewable and Sustainable Energy Reviews, 82, 2680-2692.

[21] Abiodun, O. I., Jantan, A., Omolara, A. E., Dada, K. V., Umar, A. M., Linus, O. U., ... and Kiru, M. U. (2019). Comprehensive review of artificial neural network applications to pattern recognition. IEEE Access, 7, 158820-158846.

[22] Guillod, T., Papamanolis, P., and Kolar, J. W. (2020). Artificial neural network (ANN) based fast and accurate inductor modeling and design. IEEE Open Journal of Power Electronics, 1, 284-299.

[23] Khalil, I. U., Ul-Haq, A., Mahmoud, Y., Jalal, M., Aamir, M., Ahsan, M. U., and Mehmood, K. (2020). Comparative analysis of photovoltaic faults and performance evaluation of its detection techniques. IEEE Access, 8, 26676-26700.